Response of Portable Particulate Monitoring Instruments to Combustion Particulates, Road Dust, and Salt Aerosols

Nelson Bryner, William D. Walton, Laurean DeLauter, and William Twilley
National Institute of Standards & Technology, U.S. Department of Commerce
Gaithersburg, MD USA 20899-8641
nelson.bryner@nist.gov

Joseph V. Mullin
Technology Assessment and Research Branch
Minerals Management Service, U.S. Department of Interior
Herndon, VA USA 22070

Abstract

This study examined the response of several particulate monitoring instruments to aerosols which might be encountered during monitoring of an *in situ* oil spill burn. Aerosols included road dust, salt, and particulates from the combustion of heptane, diesel fuel, and crude oil. Different sampling heads, including Total Suspended Particulates, 10 μm cutoff (PM-10), and 2.5 μm cutoff (PM 2.5), were used with each instrument. Both optical cell and gravimetric instruments reported similar concentrations of aerosols generated by combustion of crude oil, diesel fuel, or heptane. For the road dust and salt aerosols, gravimetric monitors reported mass concentrations two to three time higher than the values recorded by the optical cell instruments.

1.0 Introduction

This study examined the response of several particulate monitoring instruments to aerosols which might be encountered during monitoring of an *in situ* oil spill burn. Oil spill response teams require portable instrumentation which can quickly determine the mass concentration of airborne particulates from both ambient sources and combustion of oil during an *in situ* burn. The ability to characterize particulates from ambient sources is important because on scene commanders (OSC) typically include the concentrations of ambient particles as one of the factors that must be considered in the process of determining whether *in situ* burning is an appropriate response to a specific oil spill. Once the OSC has determined that *in situ* burning is an appropriate response, the OSC may deploy particulate instrumentation to monitor the mass concentration of particulates at various ground level locations. If particulate mass concentrations should exceed a designated level of concern, the OSC may decide that it is appropriate to terminate the *in situ* burn. It is critical that oil spill response teams understand how each instrument responds to different aerosols they may encounter on the scene of an oil spill.

Instruments which are used to monitor particulate mass concentrations often utilize either optical or gravimetric methodology. Optical cell instruments, such as

Arctic and Marine Oilspill Program (AMOP)Technical Seminar, 22nd. Environment Canada. Volume 2. Proceedings. June 2-4, 1999, Alberta, Canada, Environment Canada, Ottawa, Ontario, 519-544 pp, 1999.

the RAM-1* and DataRAM monitors (MIE Inc., Bedford MA), DustLite Monitor (Rupprecht & Patashnick Co., Albany, NY), or HAZ-DUST Monitor (SKC, Inc., Eighty Four, PA), employ an infrared light emitting diode source (~ 900 nm wavelength) and a silicon photodiode scattering detector to track the amount of light scattered by the aerosol within a sample cell. Electronics then process the scattering signal and translate the intensity of scattered light to mass concentration. These optical cells display the mass concentration of the aerosol particulates as the monitors sense the particulates. For monitoring *in situ* burning of oil spills, this type of instrument is extremely useful because they are simple to set-up in the field, battery powered, and provide real-time particulate mass concentration data.

High volume gravimetric instrumentation, such as PM-10 HiVol monitors, are designed to filter the particles from large volumes of air onto a single filter over relatively long periods, days or weeks; the resulting data are particulate masses which has been integrated over the entire collection period. This filter is periodically replaced with a fresh filter and the "used" filter is returned to a laboratory environment to be weighed. The integrated mass determined from the filter weighing is divided by the collection volume which results in an averaged value of particulate mass concentration. Although this type of equipment is easy to set up in the field, the large blower motors are not typically battery powered, and the instruments do not provide real-time particulate mass concentration data. While these analyzers are ideal to provide routine monitoring of fixed sites over long periods of time, they do not provide the portability or real-time data typically required by *in situ* burn response teams.

Low volume gravimetric monitors, such as filter cartridges coupled to small battery powered pumps, can overcome the portability issues associated with the high volume instrumentation. However, the resulting data are integrated or averaged particulate mass concentrations and do not provide real-time data for an *in situ* burn response team.

Other gravimetric instrumentation, such as the tapered element oscillating microbalances (TEOM, Rupprecht & Patashnick, Co.), can provide real-time mass concentration data. A TEOM continuously samples a small volume and collects the aerosol particulates on a filter media. However, rather than removing the filter for weighing, a TEOM utilizes an oscillating filter and as mass accumulates on the filter media, the electronics track the resulting change in frequency of oscillation. The electronics translate this change in frequency into an accumulation of mass on the filter and when divided by the sample volume, a TEOM provides real-time particulate mass concentration data. Depending on the particulate mass concentration, a TEOM filter can last for hours or weeks before it requires changing so a TEOM can be used for routine monitoring of particulates. Although a TEOM is field deployable, it does require a longer set-up time than either the optical cells or the high volume gravi-

---

* Certain trade names and company products are mentioned in the text or identified in an illustration in order to specify adequately the experimental procedure and equipment used. In no case does such identification imply recommendation or endorsement by the National Institute of Standards and Technology, nor does it imply that the products are necessarily the best available for the purpose.

metric samplers and the associated sample pump and heaters are not battery powered. And since it requires about an hour for the heaters to warm the filter and inlet sections to typical operating temperatures, it would be difficult to move the TEOM from one location to another and quickly begin collecting real-time data. This type of monitor affords real-time mass concentration data, but does not provide quick set-up and portability which is often required by an oil spill response team.

Oil spill response teams utilize optical cells precisely because optical cell based monitors are relatively small, portable, battery powered, and can provide real time particulate mass concentration data shortly after arriving on the oil spill scene. Neither type of gravimetric instrument, either the high volume or TEOM, are as portable or small as the optical cell monitors and only the TEOMs can provide real time mass concentration data. However, while the optical cells are the easiest to operate, do the optical cells measure or "see" various types of particulates equally well? Do the gravimetric instruments respond as well as the optical units do? This study was designed to examine how well optical cell and gravimetric instruments respond to different types of aerosol particulates which might be encountered by an oil spill response team.

During this study, particulate monitoring instrumentation was exposed to airborne particulates which one might encounter in background or ambient conditions as well as combustion generated aerosols. While road dust and salt particulates were aerosolized to represent ambient types of aerosols, heptane, crude oil, and diesel fuel were burned to simulate the smoke generated during an *in situ* burn. The response of the instruments was examined during laboratory and field experiments. During the first phase of this study, the aerosol particulates were generated and sampled in a small scale, controlled laboratory environment at the Large Fire Research Facility at NIST. This had the advantage of being able to conduct a wider number of combinations than the field experiments. The second phase involved field experiments at the US Coast Guard's Fire and Safety Detachment test facility on Little Sand Island, Mobile Bay, Alabama. The field experiments had the advantage of being conducted under conditions that an oil spill response team might actually encounter.

2.0 Experimental Apparatus and Procedure

The Aerosol Sampling and Measurement Apparatus (ASMA, see Figure 1) was designed to sample from a smoke plume or aerosol cloud, add particulate-free dilution air if necessary, and provide a well mixed volume of aerosol from which up to four instruments could simultaneously sample particulates. The four monitoring instruments included for this study were a RAM-1, DataRAM, and two TEOMs. Each of the instruments sampled through a number of different sampling inlets, including a total suspended particulates (TSP), a 10 μm diameter cutoff (PM-10), and a 2.5 μm diameter cutoff (PM 2.5). Small pools, less than 0.1 m diameter, of crude oil, heptane, and diesel fuel were burned to produce combustion particulates. Powdered salt (NaCl) and standard "Arizona" road dust (ISO 12103-1 A2, fine grade and ISO 12103-1 A4, coarse grade , Powder Technology, Inc., Burnsville, MN) were aerosolized by a pneumatic injection system to generate non-combustion aerosols. A dilute solution of sodium chloride was also nebulized using pressurized nitrogen.

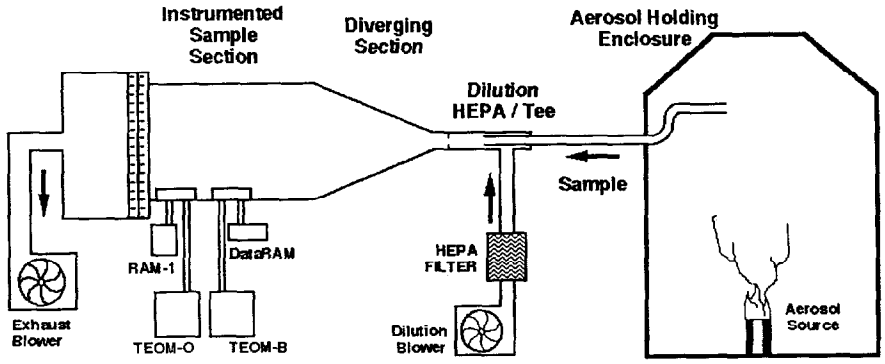

Figure 1 Aerosol Sampling and Measurement Apparatus Under Furniture Calorimeter Hood at Large Fire Research Facility

It was most important that all the instruments "see" and sample from a volume of aerosol which is uniform in terms of mass concentration, chemical composition, and physical and optical properties. While the aerosol should be as representative as possible of an aerosol a response team might monitor, the specific properties were secondary to making sure the instruments were exposed to the same aerosol. For example, while a response team is most likely to be monitoring field concentrations of less than 500 $\mu g/m^3$, it was less important whether the concentration was 400 or 600 $\mu g/m^3$, but most important that all the instruments simultaneously sampled the same concentration. The ASMA was designed to minimize particle losses due to inertial impaction and diffusion to the walls, but again, the specific mass concentration and particle size distribution of the aerosol were less critical than insuring that all the instruments sample from a aerosol that was uniform.

2.1 Aerosol Sampling and Measurement Apparatus

The Aerosol Sampling and Measurement Apparatus included a flexible sampling duct, a dilution/HEPA (High Efficiency Particulate Arrestance) filter tee, a diverging section, an instrumented sampling section, and an exhaust box (Figure 1). The sampling duct was 0.15 m (nominal) diameter flexible corrugated aluminum tubing. Three sections of duct, each 2.6 meters long for a total of 7.8 meters, were used to sample aerosol during the laboratory experiments. For the field experiments on Little Sand Island, an additional three sections for a total sampling tube length of 15.6 meters. Flexible aluminum tubing was selected to allow the sampling inlet to be quickly positioned at different locations.

The dilution /HEPA filter tee was fabricated out of a 0.2 m diameter steel duct. A small blower capable of providing up to 0.095 m^3/s of air was attached to the side port of the tee. The blower pulled the air through a prefilter and forced the air through a HEPA filter which had a Dioctyl Phthalate (DOP) filter efficiency rating of 95 percent. The blower was attached to a variable speed motor which would allow the system to provide clean dilution air at different flow rates. The blower/filter was

used to "zero" the instrumented section by providing sufficient particle free air to flood the instrument section. The variable speed blower also allowed clean dilution air to be mixed with the aerosol sample to reduce the mass concentration to lower values. The sample was drawn through the 0.15 m diameter duct which was inserted inside the 0.2 m tee. The dilution air entered through the annular area between the inner and outer ducts. A mixing ring, an orifice of 0.15 m diameter, was located 0.3 m downstream of the tee to promote complete mixing of the sample and dilution air.

The diverging section of the ASMA was fabricated out of galvanized sheet metal which was 1 m in diameter and 1.1 m in length. The diverging section provided a smooth transition between the 0.2 m diameter duct and the 1 m diameter instrumented section. Assuming the maximum volumetric flow rate of 0.095 m^3/s, the bulk average velocities at the entrance and exit of the diverging section were 2.9 m/s and 0.12 m/s, respectively.

The instrumented section was 1.2 m long by 1 m diameter and fabricated out of 1.6 mm thick galvanized sheet metal. Four openings, two located on the underside and two on the upper half provided access to install and adjust sampling probes and sample heads. End sections constructed out of 1.2 m x 1.2 m square 19 mm thick plywood were attached to the end of each section and allowed each section to be bolted together. A thin rubber gasket between the sections of plywood, prevented infiltration of air into the sampling section. A white light beam was used to probe the interior of the instrumented section while sampling heptane combustion smoke. Qualitatively, the particulates, as indicated by the back scattered white light, appeared very uniform throughout the instrumented section and this suggested that the mixing and diverging sections were providing a reasonably uniform aerosol to the instrumented section.

The two access panels on the under side of the instrumented section allowed for the insertion of probes through four sampling ports. Each of the four particulate instruments was positioned directly below the sampling head. All four of the sampling heads were placed at approximately the same elevation, 0.5 m above the centerline of the section floor. Sampling heads and instruments were rotated throughout each of the four sampling ports. Sampling tube length was kept to a minimum by moving the instruments rather than adding more sample tubing. For the RAM-1 and DataRAM, short sections of copper tubing, either 0.15 or 0.30 m long and 7.9 mm diameter, were necessary to maintain the TSP, PM -10 and PM 2.5 heads at the proper elevation. Each sampling port was at least 0.15 m from adjacent ports to help assure that upstream sampling heads would not block the flow to downstream sampling heads.

An exit plenum and exhaust blower were connected to the exit of the instrumented section. A variable speed motor/exhaust blower provided a total flow of up to 0.095 m^3/s and allowed the flow rate through the instrumented section to be reduced to approximately 0.033 m^3/s. A series of screens were installed at the entrance of the exhaust plenum to provide a resistance to the flow and promote uniform flow across the entire 1 m diameter flow cross section.

2.2 Laboratory Experiments

Several different sources of aerosols were used to test the response of the instruments. Each aerosol was generated in a Aerosol Holding Enclosure (AHE)

which had a volume of approximately 20 m^3. The entire enclosure was constructed underneath a 2.4 x 3 m combustion exhaust hood. Small fans inside the enclosure continuously mixed the aerosol within the volume. The ASMA continuously pulled a sample out of the AHE, through the instrumented section, and then recycled the aerosol to the holding enclosure. At the end of each experiment, an external hood exhaust blower was turned on and evacuated the holding enclosure.

Aerosol was generated using three different methods. For combustion aerosols, liquid fuels were burned in cylindrical burners. Typically a single 0.1 diameter cylindrical burner was used to begin each experiment. As the mass concentration exceeded approximately 500 $\mu g/m^3$, the larger burner was extinguished and two smaller diameter, 0.02 m, burners were ignited to maintain the desired concentration. For road dust and dry sodium chloride, a pre-measured amount of powder, typically 500 mg, was loaded into a 12.7 mm diameter tube. After aligning the tube parallel to the exhaust of the ASMA to enhance mixing, a volume of pressurized nitrogen was used to disperse the powder into the enclosure. Sodium chloride particulates were also generated by spraying a dilute salt solution, 32 g of sodium chloride per liter of water, into the holding enclosure. The solution was forced through a 0.1 mm diameter orifice nozzle using nitrogen pressurized to 6.9×10^5 Pa (100 psi). As the water evaporated, the residual salt formed particulates.

2.3 Particulate Monitors and Sampling Heads

Four particulate monitoring instruments simultaneously sampled the aerosol cycled through the ASMA. Two commonly used instruments, a RAM-1 and DataRAM, were chosen to represent optical cell methodology. Both of these instruments provide real time display of mass concentration in units of mg/m^3. The RAM-1 was operated on the 0 to 20 mg/m^3 scale with a 0.5 second time constant and sample and purge flows of 3.3×10^{-4} m^3/s and 3.3×10^{-5} m^3/s, respectively. The DataRAM was operated on the 0 to 4 mg/m^3 with a 1 s time constant and sample and purge flows of 3.3×10^{-5} m^3/s and 3.3×10^{-6} m^3/s, respectively. The gravimetric or filter methodology was represented by two tapered element oscillating microbalances (TEOMs). Each of the TEOMs was operated on the 0 to 20 mg/m^3 scale and sample and bypass flows of 5.5×10^{-5} m^3/s and 2.9×10^{-4} m^3/s, respectively. The TEOMs used a more complex algorithm to generate a sample averaging window which included two time constants, one for mass concentration and one for total mass. After some experimentation, values of 20 seconds and 40 seconds were selected for the mass concentration and total mass time constants, respectively.

Four types of sampling heads were used to sample the aerosol in the instrumented section. Preliminary runs were conducted with simple open tubes (0.012 m diameter copper tube) where the flow was perpendicular to the sample tip. Both the optical cells and gravimetric instruments also used heads which were designed to sample all the airborne particulates, total suspended particulates (TSP), which included the omnidirectional sample head for the RAM-1 and DataRAM as well as the TSP head for the TEOMs. The last two types of sample heads were size selective or cut-off heads. PM-10 and PM-2.5 heads were designed to collect particles with an aerodynamic diameter less than a 10 μm, and a 2.5 μm, respectively.

2.4 Data Acquisition System

A CR23X (Campbell Scientific, Inc., Logan UT) data acquisition system provided the capability to collect twelve channels of data. Typical channel assignments are listed in Table 1. In each case, the analog output from the instrument was wired directly into the datalogger. The internal averaging and datalogging capability of the DataRAM and TEOMs was not utilized for these experiments. The CR23X provided 12 bit resolution over the measurement range selected, allowed the clock time to be recorded with each data point, had sufficient internal memory for a 12 hour run, and was powered by batteries. Each of the twelve channels was scanned every 2 seconds and stored in the solid state memory of the datalogger. In addition to recording the raw data, the CR23 X software allowed the voltage signals to be corrected for zero offsets and scaled into concentration units. The raw and processed data could also be viewed in real time with the datalogger connected to a laptop computer.

Table 1 Data Channel Assignments

Channel	Analog Signal	Measurement Range
1	RAM-1	0 to 20 mg/m^3
2	DataRAM	0 to 4 mg/m^3
3	TEOM Blue High Range	0 to 20 mg/m^3
4	TEOM Orange High Range	0 to 20 mg/m^3
5	Carbon Dioxide A	0 to 1000 µmol/mol (ppm)
6	Carbon Dioxide B	0 to 1000 µmol/mol (ppm)
7	Marker Channel	0 to 5 volts
8	Ambient Temperature	273 to 1533 K
9	Sample Tube Inlet Temperature	273 to 1533 K
10	Outlet Temperature	273 to 1533 K
11	TEOM Blue Low Range	0 to 1 mg/m^3
12	TEOM Orange Low Range	0 to 1 mg/m^3

After all the instruments were zeroed and spanned, data collection was initiated and several minutes of background data were collected. This provided the operator with the opportunity to double check that each instrument was performing within manufacturer's specifications. After each run, the data was downloaded from the datalogger to the hard disk of the computer.

During the laboratory series of experiments, 124 sets of data were collected on six different aerosols as tabulated in Table 2.

2.5 Field Experiments on Little Sand Island

The ASMA was transported to Little Sand Island in Mobile Bay, Alabama and set up for field measurements. The ASMA was positioned on a rubber tired cart to provide mobility, but it still required several hours to move it from one location to another and set it up for collection (Figure 2). Each morning, the ASMA was

positioned 45 meters downwind from the center of the fire. The instrumentation was allowed to warm up and then zeroed and spanned. Data acquisition was initiated and the ASMA monitored ambient conditions until a 4.6 m diameter pool of diesel fuel was ignited. The diesel fuel burns were part of work which was evaluating a test protocol for fire-resistant oil spill containment boom.

Since the diesel fuel could only be ignited when the wind was from specific directions, there could be hours before the wind conditions were favorable for ignition of the diesel fuel. If the wind direction changed significantly from when the ASMA was set up and when it was favorable to burn, there was typically not sufficient time to relocate the ASMA to a new position in order to be directly downwind of the burning diesel fuel. During the two weeks that the ASMA was operating, it was successful in sampling from the smoke plume during about 15 percent of the diesel fuel burns. This resulted in a database that contains 20 sets of ambient or background data and 5 sets of smoke plume data (Table 2).

Table 2 Laboratory and Field Experiment Data Sets

	Aerosol	Number
Laboratory Experiments	Heptane	40
	Crude Oil	4
	Road Dust (Coarse & Fine)	49
	Salt (Dry and Wet)	15
	Ambient/Background	9
	Other: Wood Cribs Vinyl Window Assembly	7
Field Experiments	Diesel Fuel, 3 m diameter	5
	Ambient/Background	20
	Other Diesel Fuel, 0.1 m dia. Ferrocene and Diesel Fuel, 4.6m dia. Tek Flame (Exxon Inc.)	8

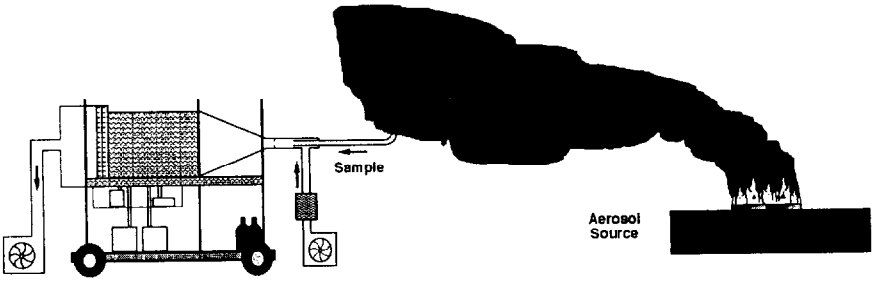

Figure 2 Aerosol Sampling and Measurement Apparatus on Little Sand Island

3.0 Results

For each experimental run, the mass concentrations of particulates for both optical and gravimetric instruments were plotted versus time. The optical instrument data were plotted as lines with every fifth data point indicated by a symbol, open circles for RAM-1 data and filled circles for DataRAM data. The gravimetric analyzer data were plotted as lines with every fifth data point indicated by a symbol, open triangles for TEOM-B data and filled triangles for TEOM-O data. For both the laboratory experiments and the field work, the graphs present data collected using the TSP, PM-10, and PM 2.5 sampling heads. While the laboratory aerosols were generated by burning crude oil and heptane and aerosolizing road dust and powdered salt, and spraying dilute salt solution, the field work only includes particulates from burning diesel fuel. This report will focus on the instrument response to combustion generated particulates, fine road dust, and dry salt aerosols. Typical plots of mass concentrations of particulates for HEPA filtered air or "zero" air is included as well as graphs of ambient background aerosols for both laboratory and field work.

3.1 Laboratory Experimental Results

The mass concentration versus time for HEPA filtered or "zero" was plotted in Figure 3 for both optical and gravimetric instruments. Averages for the mass concentration for each instrument over the 900 seconds plotted in Figure 3 results were tabulated in Table 3.

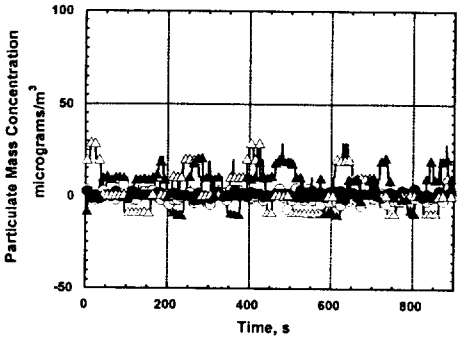

Figure 3 Mass Concentration Versus Time for HEPA Filtered or "Zero" Air

Background or ambient mass concentrations of particulates in the combustion laboratory was graphed in Figure 4 for all instruments. The background concentrations of the airborne particulates varied with the activity within the Large Fire Research Facility. During periods of low activity, average mass concentrations were lower than those plotted in Figure 4. If construction of future experiments or other burn tests were occurring within the burn facility, then average ambient particulate mass concentrations could exceed 100 $\mu g/m^3$. Experiments for this study

were not initiated if background concentrations of particulates were above 60 μg/m³. The concentrations in Figure 4 were collected during an early afternoon period with moderate construction activity and the data are representative of a typical work day. Averages for the mass concentration for each instrument over the 900 seconds plotted in Figure 4 were also tabulated in Table 3.

Table 3 Average and Standard Deviations for HEPA and Ambient Background Air Mass Concentrations

	HEPA Filtered Air (Figure 3)			Ambient Background Air (Figure 4)		
	Sample Head	Average Mass Conc. μg/m³	Standard Deviation μg/m³	Sample Head	Average Mass Conc. μg/m³	Standard Deviation μg/m³
RAM-1	PM-2.5	-1	2	PM-2.5	38	3
DataRAM	TSP	0	1	PM-10	55	3
TEOM -B	TSP	11	12	PM-10	26	12
TEOM -O	PM-2.5	6	5	PM-2.5	27	10

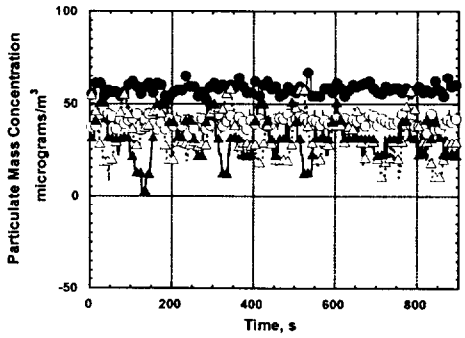

Figure 4 Ambient Aerosol Mass Concentrations Versus Time for Laboratory Environment

Mass concentrations of particulates for heptane combustion, road dust, and salt for instruments sampling with TSP sampling heads were plotted in Figures 5, 6, and 7, respectively. The DataRAM and TEOM-B tracked each other quite well for aerosols generated by combustion of heptane. Peak concentration for this test was approximately 500 μg/m³. While the peak mass concentrations for road dust and salt aerosols (Figure 6 and 7) were of similar magnitudes, the TEOM-B consistently reported higher mass concentrations of aerosol than did the DataRAM. For the road dust, the TEOM-O values were at least a factor of two higher than the DataRAM. This difference can also be observed in the powdered salt aerosols where the TEOM-

O values were a factor of two to three higher than the DataRAM. Three different injections of powdered salt were plotted in Figure 7.

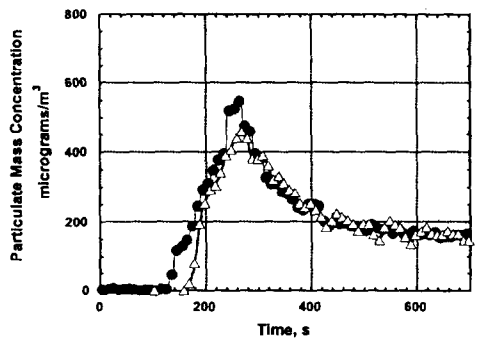

Figure 5 Mass Concentration Versus Time for Combustion of Heptane for a TSP Sampling Head

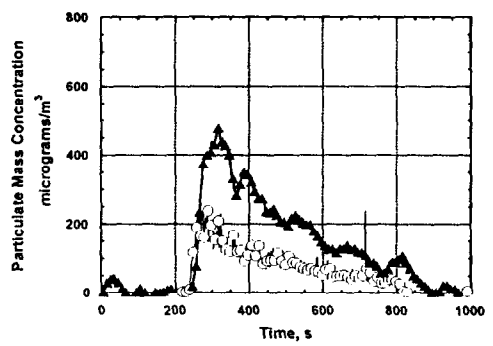

Figure 6 Mass Concentration Versus Time for Single Dispersion of Fine Road Dust for a TSP Sampling Head

Mass concentrations of particulates for heptane and crude oil combustion, road dust, and salt for instruments sampling with PM-10 sampling heads were graphed in Figures 8, 9, 10, and 11, respectively. Again the DataRAM and TEOM-B tracked each other quite well for aerosols generated by combustion of heptane. Peak concentration for this test was approximately 600 $\mu g/m^3$. For a second aerosol generated by combustion, Cook Inlet crude oil, the DataRAM responded slightly quicker than the TEOM-B, but both instruments tracked rather well with peak concentrations of 300 $\mu g/m^3$. It should be noted that at approximately 300 seconds, filtered air was introduced to dilute the combustion aerosol in order to reduce the concentration from 300 $\mu g/m^3$ to around 100 $\mu g/m^3$.

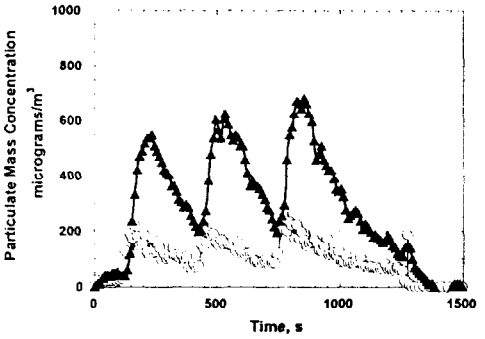

Figure 7 Mass Concentration Versus Time for Three Consecutive Dispersions of Powdered Salt for TSP Sampling Head

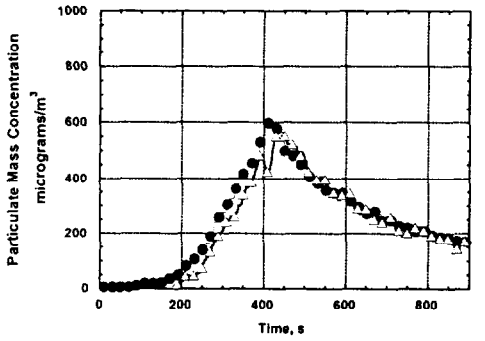

Figure 8 Mass Concentration Versus Time for Heptane Combustion Aerosols For PM-10 Sampling Head

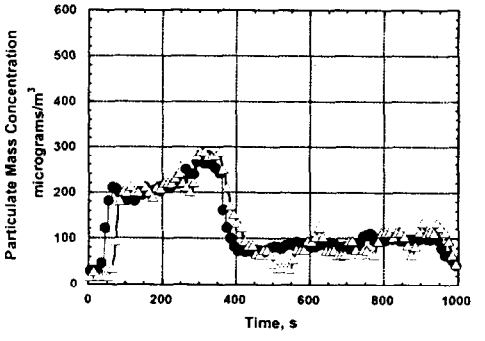

Figure 9 Mass Concentration Versus Time for Cook Inlet Crude Oil Combustion for PM-10 Sampling Head

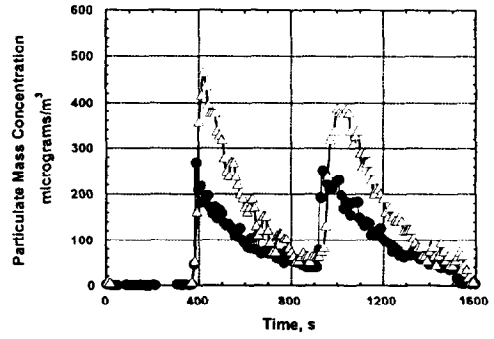

Figure 10 Mass Concentration Versus Time for Two Consecutive Dispersions of Fine Road Dust for PM-10 Sampling Head

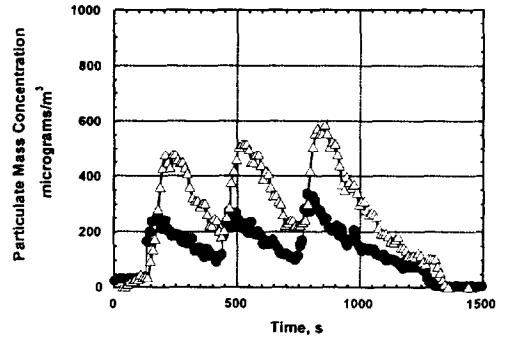

Figure 11 Mass Concentration Versus Time for Three Consecutive Dispersions of Powdered Salt for PM-10 Sampling Head

While the peak mass concentrations for road dust and salt aerosols (Figure 10 and 11) were of similar magnitudes, the TEOM-B consistently reported higher mass concentrations of aerosol than did the DataRAM. For the road dust, the TEOM-O values were at least a factor of two higher than the DataRAM. This difference can also be observed in the powdered salt aerosols where the TEOM-O values were a factor of two to three higher than the DataRAM.

Mass concentrations of particulates for heptane and crude oil combustion, road dust, and salt for instruments sampling with PM-2.5 sampling heads were plotted in Figures 12, 13, 14, and 15, respectively. Again the DataRAM and TEOM-B tracked each other quite well for aerosols generated by combustion of heptane. Peak concentration for this test was approximately 350 $\mu g/m^3$. For a second aerosol generated by combustion, Cook Inlet crude oil, the DataRAM responded slightly quicker than the TEOM-B, but both instruments tracked rather well with peak concentrations of 700 $\mu g/m^3$.

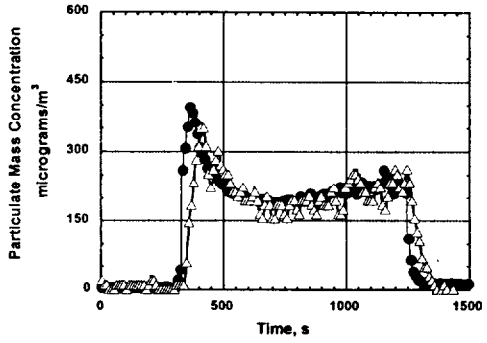

Figure 12 Mass Concentration Versus Time for Heptane Combustion Aerosols For PM-2.5 Sampling Head

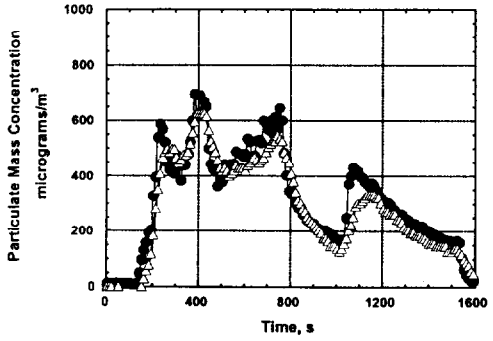

Figure 13 Mass Concentration Versus Time for Cook Inlet Crude Oil Combustion for PM-2.5 Sampling Head

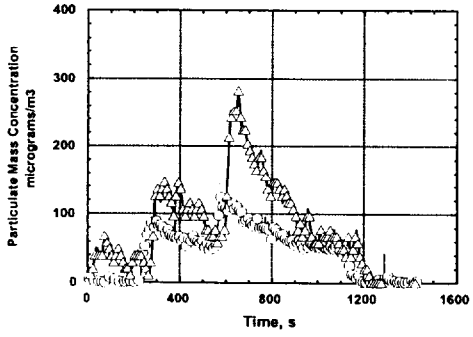

Figure 14 Mass Concentration Versus Time for Two Consecutive Dispersions of Fine Road Dust for PM 2.5 Sampling Head

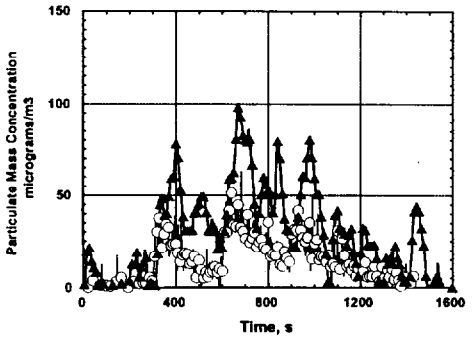

Figure 15 Mass Concentration Versus Time for Two Consecutive Dispersions of Powdered Salt for PM-2.5 Sampling Head

3.2 Field Experimental Results

The series of experiments conducted on Little Sand Island provided a smaller number of data sets. Mass concentrations of particulates for HEPA filtered air or zero air were plotted in Figure 16 for all four instruments. The "zeroes" for the field work were higher than for the laboratory experiments. Mass concentrations of ambient or background aerosols were graphed in Figure 17. While the gravimetric monitors produced a much noisier signal than the optical cells, all average concentrations were less than 50 $\mu g/m^3$. Average concentrations and standard deviations for each of the four monitors (two plotted in Fig. 17 and two not included) are tabulated in Table 4.

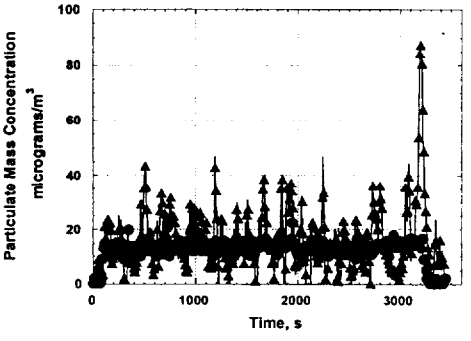

Figure 16 HEPA Filter Air Aerosol Mass Concentration Versus Time For Field Experiment On Little Sand Island

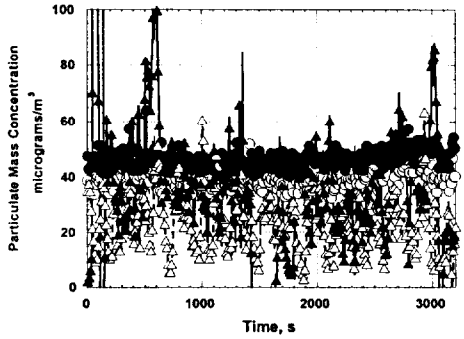

Figure 17 Ambient Air Aerosol Mass Concentration Versus Time For Field Experiment On Little Sand Island

Table 4 Average and Standard Deviations for HEPA and Ambient Background Air Mass Concentrations On Little Sand Island

	HEPA Filtered Air (Figure 16)			Ambient Background Air (Figure 17)		
	Sample Head	Average Mass Conc. $\mu g/m^3$	Standard Deviation $\mu g/m^3$	Sample Head	Average Mass Conc. $\mu g/m^3$	Standard Deviation $\mu g/m^3$
RAM-1	TSP	12	5	TSP	40	5
DataRAM	PM-10	12	4	PM-10	46	3
TEOM -B	TSP	16	15	TSP	24	9
TEOM -O	PM-10	16	12	PM-10	36	25

Mass concentrations of particulates for diesel fuel for instruments sampling with TSP, PM-10, and PM-2.5 sampling heads were plotted in Figures 18, 19, and 20, respectively. The TSP and PM-10 data sets were collected from the same fire while the PM-2.5 data set was collected from a different fire. The sampling inlet of the ASMA was fixed and as the wind changed direction it would cause the smoke plume to sweep across the inlet which allowed the instruments to monitor the mass concentration. Dilution air was not added during the field experiments. The optical cells and gravimetric monitors tracked each other relatively well. Both the optical cells, RAM-1 (Figure 18 and 19) and DataRAM (Figure 20), appeared to respond slightly more quickly than the gravimetric instruments. The data from the optical cells resulted in higher, but narrower peaks in mass concentration while the gravimetric data appeared to have shorter, smoother, and slightly wider peaks. This would be consistent with the slightly longer averaging time which was employed by the TEOMs. Peak concentration for the TSP and PM-10 sampling heads, Figures 18 and 19, were approximately 3000 $\mu g/m^3$ for the optical cells and about 1000 $\mu g/m^3$ for the TEOMs . For the PM-2.5 sampling head data set the peak mass concentrations exceeded 8000 $\mu g/m^3$ for both optical and gravimetric instruments. Although the mass concentration of ambient particulates was similar in the laboratory and field

work, the field experiments sampled much higher concentrations of smoke particulates than did the laboratory experiments.

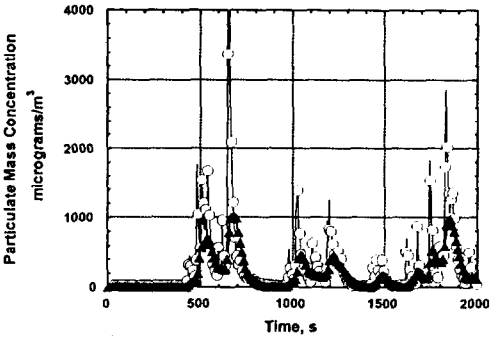

Figure 18 Mass Concentration Versus Time For Diesel Fuel Combustion For Field Experiment On Little Sand Island Using TSP Sampling Head

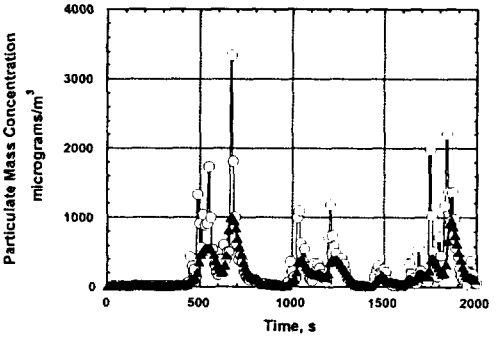

Figure 19 Mass Concentration Versus Time For Diesel Fuel Combustion For Experiment on Little Sand Island Using PM-10 Sampling Head

Comparison of the mass concentrations based on the TEOMs results with TSP, PM-10, and PM-2.5 heads indicates that most of the combustion generated smoke particulates were less than 2.5 μm in diameter. In Figure 21, the mass concentration data from two TEOMs, one sampling with a TSP head and the other with a PM-10 head, were plotted for heptane combustion. Since the mass concentration reported by the TEOM sampling with the TSP was not significantly higher than the TEOM with the PM-10 head, it would be consistent with the suggestion that most of the particulates are PM-10 size or less. For a different experiment, the mass concentration data from a TEOM sampling with a PM-10 head

while a second samples with a PM-2.5 head (Figure 22). Again the mass concentrations appear similar and this would be consistent with most of the particulates being PM-2.5 size or less. This comparison was repeated for burning crude oil in Figures 23 (TSP versus PM-10) and 24 (PM-10 versus PM-2.5). For the TSP versus PM-10 data in Figure 23, the mass concentrations appeared similar until the concentrations decreased to around 100 $\mu g/m^3$ then the TSP did appear slightly higher than the PM-10 data. It is not clear whether this difference is significant, but may indicate the presence of some larger particulates. In Figure 24 for crude oil aerosols, the mass concentrations appeared similar and this was consistent with most of the particulates that were less than PM-10 size were also less than PM-2.5 size.

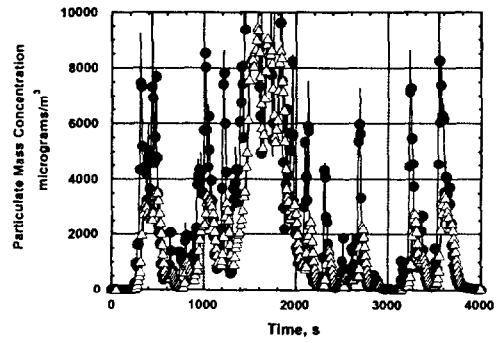

Figure 20 Mass Concentration Versus Time For Diesel Fuel Combustion For Experiment on Little Sand Island Using PM-2.5 Sampling Head

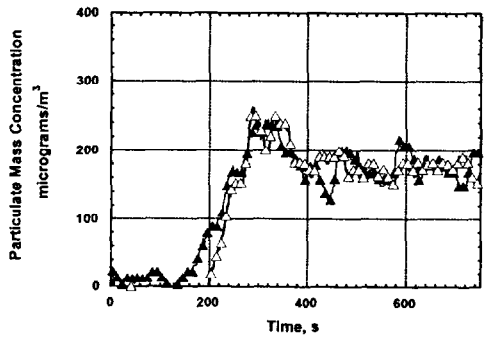

Figure 21 Mass Concentration Versus Time for Heptane Combustion Aerosols Comparing TSP and PM-10 Sampling Heads

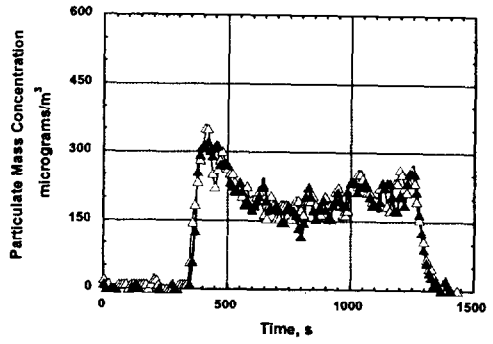

Figure 22 Mass Concentrations Versus Time for Heptane Combustion Aerosols Comparing PM-10 and PM-2.5 Sampling Heads

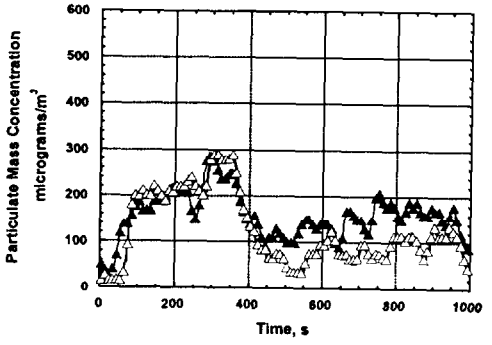

Figure 23 Mass Concentration Versus Time for Crude Oil Combustion Aerosols Comparing TSP and PM-10 Sampling Heads

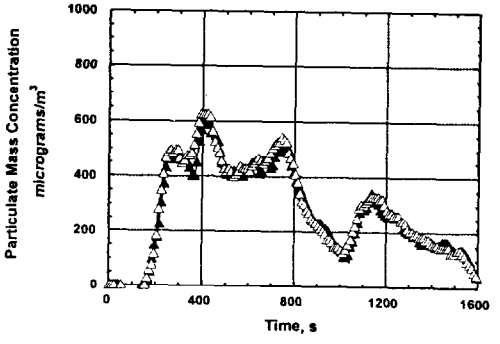

Figure 24 Mass Concentrations Versus Time for Crude Oil Combustion Aerosols Comparing PM-10 and PM-2.5 Sampling Heads

4.0 Uncertainty Analysis

There are many different components of uncertainty in the mass concentration data reported here. Uncertainties are grouped into two categories according to the method used to estimate them. Type A uncertainties are those which are evaluated by statistical methods, and Type B are those which are evaluated by other means (Taylor and Kuyatt, 1994). Type B analysis of systematic uncertainties involves estimating the upper ($\overline{x}$ + a) and lower ($\overline{x}$ - a) limits for the quantity in question such that the probability that the value would be in the interval ($\overline{x}$ ± a) is essentially 100 percent. After estimating uncertainties by either Type A or B analysis, the uncertainties are combined in quadrature to yield the combined standard uncertainty. Multiplying the combined standard uncertainty by a coverage factor of two results in the expanded uncertainty which corresponds to a 95 percent confidence interval(2σ).

Components of uncertainty are tabulated in Table 5, 6 and 7. The uncertainties were computed for an arbitrary aerosol with mass concentration less than 500 $\mu g/m^3$, at 300 K, at 101,325 Pa, and containing road dust, combustion soot, and salt. Resulting uncertainty in mass concentration (columns 3 & 5 in Tables 5 and 6 and column 3 in Table 7) is before combination by quadrature and does not include coverage factor. Some of these components, such as the zero, span, and mass calibration elements, are derived from instrument specifications. Other components, such as volume and purge/window flows, include past experience using flow calibrators and stopwatches. The temperature, pressure, and humidity components include effects of typical operating conditions, up to a 12 K shift in temperature (298 K to 310 K), pressure fluctuations of 2000 Pa (15 mm Hg), or varying humidity. While the humidity component considers the dilution effect of added moisture in the sample (thus possibly lowering mass concentrations), it does not try to assess uncertainty arising from condensation on particulates (optical cells) or adsorption onto filter media (gravimetric monitors). Moisture condensation and adsorption effects can be mitigated by using in-line heaters which are standard equipment on the Series 1400 TEOMs and can be added to the sampling train for the RAM-1 and DataRAM.

Loss of particulates to sample train walls is a function of particle velocity, diameter, shape, size, and charge as well as sample tube diameter, bends in the sample lines, material, and length. Stenger and Bajura (1984) reported particle losses in a high temperature probe of up to 15 percent. Lui *et al.* (1986) demonstrated that particle losses to walls could range up to 100 percent, but their work included electrostatically charged particles in non-conductive tubing. Since the sample tubing for the optical cells was copper and short, the sample temperatures were near ambient, and the aerosol was quite dilute and probably had a relatively small average diameter, the uncertainty associated with wall losses was estimated to be approximately 10 percent for the RAM-1 and DataRAM. In addition to the short sampling length, and dilute, small diameter aerosol, the TEOM walls were heated at 323 K, and there were no bends or turns upstream of the filter, so the uncertainty associated with wall losses was estimated to be about 7.5 percent for the TEOM.

Table 5 Uncertainty Components for Mass Concentration Data for RAM-1and DataRAM

Component	RAM-1		DataRam	
	Component Standard Uncertainty	Resulting Uncertainty Mass Conc. $\mu g/m^3$	Component Standard Uncertainty	Resulting Uncertainty Mass Conc. $\mu g/m^3$
Zero Calibration	± 3.5 %	± 18	± 3 %	± 15
Span Calibration	± 3.5 %	± 18	± 3 %	± 15
Purge Flow	± 3.5 %	± 18	± 3 %	± 15
Wall Losses	-0 % + 10 %	-0 + 50	- 0 % + 10 %	-0 + 50
Size Distribution	- 5% + 70%	- 25 + 350	- 5% + 70%	- 25 + 350
Refractive Index	± 15 %	± 75	± 15 %	± 75
Random*	± 2 %	± 10	± 2 %	± 10
Repeatibility	± 5 %	± 25	± 5 %	± 25
Combined Standard Uncertainty	- 18 % + 73 %	- 90 + 365	- 18 % + 73 %	- 90 + 365
Total Expanded Uncertainty	- 36 % + 145 %	- 180 +730	- 36 % + 145 %	- 180 + 730

Notes:
* Random component evaluated as Type A, other components as Type B.

Table 6 Uncertainty Components for Mass Concentration Data for calibrated RAM-1and DataRAM

Component	RAM-1		DataRam	
	Component Standard Uncertainty	Resulting Uncertainty Mass Conc. $\mu g/m^3$	Component Standard Uncertainty	Resulting Uncertainty Mass Conc. $\mu g/m^3$
Zero Calibration	± 3.5 %	± 18	± 3 %	± 15
Span Calibration	± 3.5 %	± 18	± 3 %	± 15
Purge Flow	± 3.5 %	± 18	± 3 %	± 15
Wall Losses	-0 % + 10 %	-0 + 50	- 0 % + 10 %	-0 + 50
Random*	± 2 %	± 10	± 2 %	± 10
Repeatibility	± 5 %	± 25	± 5 %	± 25
Combined Standard Uncertainty	- 8 % + 13 %	- 40 + 65	- 8 % + 13 %	- 40 + 65
Total Expanded Uncertainty	- 16 % + 26 %	- 80 + 130	- 16 % + 26 %	- 80 + 130

Notes:
* Random component evaluated as Type A, other components as Type B.

Three of the uncertainties, size distribution, refractive index, and desorption of volatile organic hydrocarbons are more difficult to quantify, but are the largest sources of uncertainty. The intensity of light scattered from a particle is dependent on the size and refractive index of the particle. RAM-1 and DataRAM instrument specifications indicate that these optical cells responded relatively well to particles between 0.3 to 2 μm in diameter. However, the responsiveness of these instruments drops off if the particle diameter is either larger or smaller than this range. If the aerosol contains some larger particles (greater 2 μm diameter), these particle could constitute a significant portion of the aerosol mass, but not be "seen" very well by the optical cells. Instrument specification indicate that the relative response of these optical cells decreases from about 1 to 0.3 as the diameter increase from 2 to 4 μm. The uncertainty in the impact of size distribution was estimated at 70 percent for the larger particles. The refractive index of a material affects how much light is scattered or absorbed. Ice or salt (NaCl) crystals scatter or reflect almost all light while carbon particles will absorb some fraction of light (Reist 1984) . The impact of refractive index was estimated to be about 30 percent after simulating the scattering from a single spherical particle using a Mie scattering algorithm (Bohren and Huffman, 1983) for a range of refractive indices.

The desorption of organic compounds which are initially intercepted by a filter media occurs as additional air is pulled through a filter. The high volatility or vapor pressure of some organic compounds may cause some compounds to sublimate/evaporate slowly and disappear from a filter (Benner *et al.* 1990, Lillenfield 1995). This results in a lower mass on the filter which is interpreted as a lower mass concentration. Benner *et al.* reported that between 3 and 86 percent of five specific organic compounds were collected on a foam filter which was placed immediately downstream of an initial filter. Since the TEOMs were operated at a lower temperature (than Benner *et al.*) and the high volatility organic compounds represented a small fraction of the mass collected on the filter, the uncertainty due to desorption of the organic compounds was estimated at 2 percent.

The total expanded uncertainty computed for the RAM-1 and DataRAM was - 36 % to + 145 % (Table 5). The two largest contributors to this uncertainty are the effects of size distribution and refractive index. The impact of size distribution and refractive index on the mass concentration determinations by the optical cells can be minimized by careful calibration of each monitor with aerosols of similar size distribution and refractive index to that of the aerosols to be monitored. If the optical cells have been carefully calibrated to minimize or eliminate these two uncertainties, then the total expanded uncertainty for the RAM-1 and DataRAM decreases to -16 % + 26 % (Table 6). The total expanded uncertainty computed for the TEOMs was - 13 % to + 23 % (Table 7).

cells. The TEOMs would register the mass of the larger particles and the optical cells would appear to under report the mass concentration. However, this effect of a few large particles should be more apparent with the TSP and PM-10 data and less apparent with the PM 2.5 data because the PM 2.5 sampling head should prevent the large particles from entering the optical cells. There is a hint of this trend when the TSP (Figures 6 & 7), PM-10 (Figures 10 and 11), and PM 2.5 (Figures 14 and 15) for road dust and salt are compared, but it is not conclusive. How sharply the PM-10 and PM 2.5 heads cut-off or prevent the large particles from being sampled directly effects whether this trend would be visible. If the PM-2.5 cut-off is not reasonably sharp, then even a few larger particles could bias the measurements significantly.

Can correction factors be used to reduce the effect of factors such as different size distributions or refractive indices? If the monitoring instruments are calibrated against an aerosol of known size distribution, composition, and refractive index, then it should be possible to derive a correction factor. The data sets reported here begin to provide an indication as to the order of magnitude of such a correction factor. For this very limited set of data, a qualitative estimate of the correction factor would place it in the range of 1.5 to 2.5. A more generalized "correction factor" would require generating an aerosol, isolating a specific "slice" or fraction of the size distribution and then sampling the slice using an array of monitors in order to provide the response of each instrument to each fraction of the size distribution. This would need to be repeated for combustion particulates and typical components of atmospheric aerosols including soil dust, sulfates, nitrates, diesel and auto exhaust, cement dust, and sea salt (Friedlander, 1977). It is not clear how practical such a generalized correction factor would be since a response team would not know ahead of time the composition or size distribution of the aerosols at an incident site.

It may be more practical for each response team to calibrate each of their optical cells with a more limited number of aerosols (soil dust, auto and diesel soot, and combustion particulates) for three different size distributions (d_{avg} = 0.3, 1.0, and 4 μm). An aerosol sampling apparatus like the ASMA could provide a uniform sampling volume for each monitor to be run head-to-head with gravimetric monitors such as the TEOM. This would help each team better understand the performance of their monitors when sampling different aerosols.

The total expanded uncertainty (2 σ) associated with a carefully calibrated RAM-1, DataRAM, and TEOM was computed at -16 % +26 %, - 16 % + 26 %, and - 13 % + 23 %, respectively. If the optical cells have not been calibrated using aerosols similar in size distribution and refractive index to the aerosols to be monitored, the total expanded uncertainty increases dramatically to -36 % +145 % for both the RAM-1 and DataRAM. These increases point out the need for optical cells to be calibrated carefully with aerosols similar to the ones that are going to be monitored.

Each of the four monitors sampled aersols using TSP, PM-10, and PM 2.5 sampling heads. Comparing the data from TSP, PM-10 and PM 2.5 sampling heads suggests that the combustion aerosols were mostly smaller particulates less than 2.5 μm. This could help explain why the optical cells and gravimetric instruments responded equally since there were probably fewer large particles to bias the optical cell measurements.

During this study, the response of the instruments to laboratory generated aerosols appeared to be identical to the response to similar aerosols in the field. The

Table 7 Uncertainty Components for Mass Concentration Data for TEOM

Component	TEOM	
	Component Standard Uncertainty	Resulting Uncertainty in Mass Conc. $\mu g/m^3$
Mass Calibration	± 2 %	± 10
Volume	± 2 %	± 10
Desorption of Organics	- 0 % + 2 %	- 0 + 10
Wall Losses	-0 % + 7.5 %	-0 + 38
Humidity	-0 % + 4 %	-0 + 20
Pressure	± 2 %	± 10
Temperature	-0 % + 4 %	-0 + 20
Random*	± 4 %	± 20
Repeatibility	± 5 %	± 25
Combined Standard Uncertainty	- 7 % + 12 %	- 35 + 60
Total Expanded Uncertainty	- 13 % + 23 %	- 70 + 120

Notes:
* Random component evaluated as Type A, other components as Type B.

5.0 Discussion

The data sets demonstrate the response of two optical cell instruments and two gravimetric monitors to combustion aerosols, road dust, and salt particles when sampled with TSP, PM-10, and PM-2.5 sampling heads. The RAM-1, DataRAM, and both TEOMs responded equally well to aerosol particulates generated by combustion of heptane, diesel fuel, and crude oil. The data sets also indicate that optical cells and gravimetric monitors did not respond equally to road dust and salt particulates. For the road dust and salt aerosols, gravimetric monitors reported mass concentrations two to three time higher than the values recorded by the optical cell instruments. It is perhaps fortuitous that all the monitors respond equally to combustion generated particulates since the oil spill response teams would be most interested in monitoring combustion generated aerosols from an *in situ* burn. However, it is still important for the response team to understand how well their instruments "see" background aerosols as well as the combustion generated particulates. The performance of the optical cells is interesting because the optical cells are typically calibrated at the factory using "Arizona" road dust.

It is not clear why the optical cells report lower values for road dust and salt for all three sampling heads. A possible explanation for optical cells report could be different size distributions. If as the instrument specifications suggest, the RAM-1 and DataRAM are optimized for a smaller size distribution that the size distribution of the salt and road dust aerosolized during this study, then a few large particles could constitute a significant fraction of the mass, but not be "seen" well by the optical

difficulty in positioning the TEOMs under the smoke plume reinforced the feeling that TEOMs are field deployable, but not nearly as portable as the RAM-1 or DataRAM.

6.0 Conclusions

For combustion generated aerosols from burning heptane, diesel fuel and crude oil, two optical cells reported similar concentrations as those determined by gravimetric instruments. For salt and road dust aerosols, two optical cells reported much lower values than those measured by gravimetric instruments. The differences in response to salt and road dust aerosols may have resulted from the aerosols having different size distributions, but these differences may be minimized through careful calibration procedures.

With careful calibration, and daily zeroing and spanning, optical cells and gravimetric instruments can provide accurate mass concentration data for a range of aerosol particulates using TSP, PM-10, and PM-2.5 sampling heads. Whether in the laboratory at NIST or in the field on Little Sand Island, the response of the instruments to similar aerosols appeared identical.

The results of this study indicate that any of these instruments, a RAM-1, a DataRAM or a TEOM, can be used as a monitoring tool to help response teams to assess whether *in situ* burning is leading to an increase in the airborne particulate concentration above an acceptable level.

7.0 Acknowledgements

This work was funded by the Technology Assessment and Research Branch, Minerals Management Service, U.S. Department of Interior.

Dave Beene of the Marine Fire and Safety Research Branch at the U.S. Coast Guard Research and Development Center (Groton, CT) and the Fire and Safety Test Detachment in Mobile under the direction of Chief Warrant Officers Byrd and Smith provided assistance in preparing for and conducting the experiments.

Gary Roadarmel and Jack Lee provided critical operational support for the laboratory experiments conducted at the Large Fire Research Facility at NIST.

8.0 References

Benner, B.A., N.P. Bryner, S.A. Wise, G.W. Mulholland, R.C. Lao, and M.F. Fingas, "Polycyclic Aromatic Hydrocarbon Emissions from the Combustion of Crude Oil on Water", *Environmental Science and Technology,* Vol. 24, pp. 1418-1427, 1990.

Bohren, C. F., and D.R. Huffman, *Absorption and Scattering of Light by Small Particles*, Wiley-Interscience Publication, New York, NY, 530 p., 1983.

Friedlander, S. K., *Smoke, Dust and Haze; Fundamentals of Aerosol Behavior*, Wiley and Sons, New York, NY, 317 p., 1977.

Lilienfeld, P., "Nephelometry, an Ideal PM-2.5/10 Method", *Proceedings of the International Specialty Conference,* Air and Waste Management Association, Pittsburgh, PA, pp. 211-223, April 4-6, 1995.

Lui, B.Y.H., D.Y.H. Pui, K.L. Rubow., and W. W. Szymanski, "Electrostatic Effects in Aerosol Sampling and Filtration", *Ann. Occup. Hyg.*, Vol. 29. No. 2, pp. 251-269, 1986.

Reist, P. C., *Introduction to Aerosol Science*, Macmillan Publishing Company, New York, NY, 299 p., 1984.

Stenger, J.B. and R.A. Bajura, "Deposition in Sampling Tubes", *Aerosols, Science, Technology, and Industrial Applications of Airborne Particles:, Proceedings of the first International Aerosol Conference* , Elsevier, New York, NY, pp. 175-178, 1984.

Taylor, B. N. and C. E. Kuyatt, *Guidelines For Evaluating and Expressing the Uncertainty of NIST Measurement Results*. National Institute of Standards and Technology (U.S.) NIST-TN 1297; September, 20 p. 1994.